

Supporting Information

Method: Adding the litter hydrological module

First, we collect litter mass, maximum litter water content, and LAI from published articles to build a regression to describe the relationship between litter water content, litter mass, and LAI (Figure S1). Then, we simplified the litter water process and set it as a supplement to the soil water process by changing the soil depth. The explicit information is described by the following equation:

$$RSD = \frac{MLWC + MSWC}{MSWC} \times SD \quad (S1)$$

where SD is effective soil depth; RSD is the revised effective soil depth; $MLWC$ is the maximum litter water content; and $MSWC$ is the maximum soil water content.

$$VWC_{SAT} = \frac{(50.5 - 0.142 \times sand - 0.037 \times clay)}{100} \quad (S2)$$

$$MSWC = SD \times VWC_{SAT} \times 1000 \quad (S3)$$

where VWC_{SAT} is the volumetric water content at saturation; $sand$ is the ratio of the sand content; and $clay$ is the ratio of the clay content.

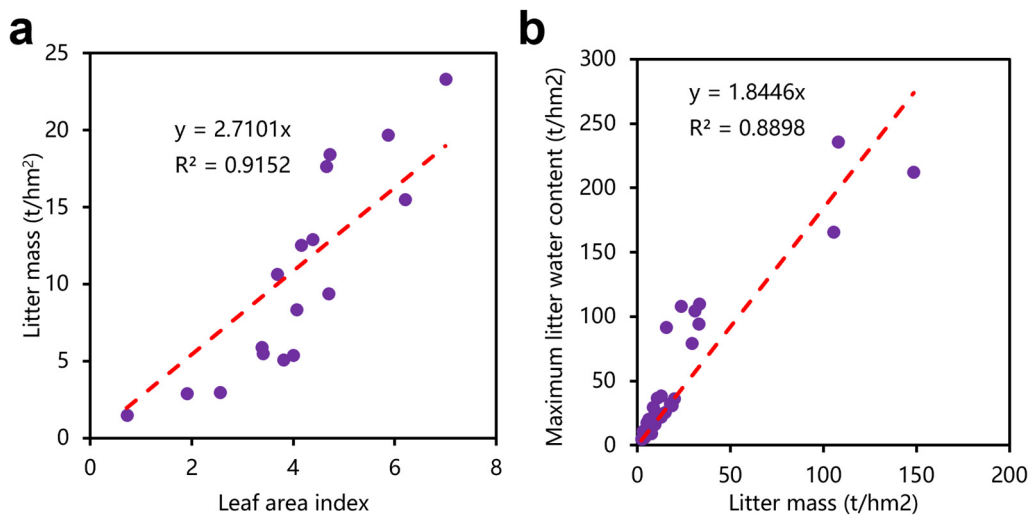


Figure S1. a) Correlation between LAI and litter mass; b) correlation between litter mass and maximum litter water content.

Table S1. LULC categories.

Categories	Sub-categories
Forest	Evergreen Needleleaf Forest Deciduous Needleleaf Forest Deciduous Broadleaf Forest Shrubland
Grassland	Grassland
Wetland	Wetland
Cropland	Cropland
Urban	Settlement Transportation land Mining field

Table S2. Eco-physiological parameters of the Biome-BGC model

Parameters	ENF	DBF	DNF	Shrub	Grass	Cropland
C:N of leaves	46	16.58	24.0	35	23.37	65
C:N of leaf litter	93	49	49.0	75	45 ^g	85
C:N of fine roots	90	43.2	42.0	58	23.37	120
C:N of live wood	50	50	50.0	50	-	-
C:N of dead wood	729	550	442.0	730	-	-
Leaf litter labile proportion	0.32	0.20	0.39	0.3	0.29	0.68 ^g
Leaf litter cellulose proportion	0.44	0.51	0.44	0.45	0.55	0.23 ^g
Leaf litter lignin proportion	0.24	0.29	0.17	0.25	0.16	0.09 ^g
Fine root labile proportion	0.30	0.12	0.30	0.34	0.34 ^g	0.34
Fine root cellulose proportion	0.45	0.54	0.45	0.44	0.44 ^g	0.44
Fine root lignin proportion	0.25	0.34	0.25	0.22	0.22 ^g	0.22
Dead wood cellulose proportion	0.76	0.78	0.76	0.71	0.75 ^g	0.75 ^g
Dead wood lignin proportion	0.24	0.22	0.24	0.29	0.25 ^g	0.25 ^g
Water interception coefficient ($\text{LAI}^{-1} \text{ day}^{-1}$)	0.041	0.0355	0.041	0.045	0.027 ^g	0.027 ^g
Light extinction coefficient	0.5	0.599	0.5	0.55	0.60	0.48
All-sided to projected leaf area ratio	2.6	2	2.6	2.3	2.0 ^g	2.0 ^g
SLA (projected area basis) ($\text{m}^2 \text{ kg}^{-1} \text{ C}$)	12.0	46.64	30.0	25.98	11.88	2.0 ^g
Ratio of shaded SLA: sunlit SLA	2.0	2.0	2.0	2.0	2.0 ^g	2.0 ^g
maximum stomatal conductance	0.0022	0.0094	0.005	0.006	0.006 ^g	0.006 ^g
Cuticular conductance (m s^{-1})	0.00001	0.000094	0.00001	0.00006	0.00006 ^g	0.00006 ^g
Boundary layer conductance (m s^{-1})	0.08	0.01	0.08	0.02	0.04	0.003
LWP _i	-0.6	-0.34	-0.6 ^g	-0.81	-0.42	-0.42 ^g
LWP _f	-2.3	-2.2	-2.3 ^g	-4.2	-0.42	-2.7 ^g
VPD: start of conductance reduction	930.0	1100	930.0	970	1000 ^g	1000 ^g
VPD: complete conductance reduction	4100.0	3600	4100.0	4100	5000 ^g	5000 ^g
Reference	a	b	c	d	e	f

ENF: Evergreen needleleaf forest; DBF: Deciduous broadleaf forest; DNF: Deciduous needleleaf forest;

LWP_i: leaf water potential: start of conductance reduction

LWP_f: leaf water potential: complete conductance reduction

a: Yan et al. 2016

b: Kang et al. 2019

c: Li et al. 2018

d: Zhang et al. 2015

e: Du et al. 2021

f: Xu et al. 2017

g: White et al. 2000

- Yan, M., X. Tian, Z. Li, E. Chen, C. Li, and W. Fan. 2016a. A long-term simulation of forest carbon fluxes over the Qilian Mountains. International Journal of Applied Earth Observation and Geoinformation 52:515-526.
- Kang M C, Zhu L P, Xu H, Zha T G, Zhang Z Q. Modelling the responses of carbon and water fluxes with climate change for a poplar plantation in northern China based on the Biome-BGC model. Acta Ecologica Sinica, 2019, 39(7): 2378-2390.
- Li S H, Hou L, Shi A R, Chen L, Zhu X L, Bai H Y. Response of Larix chinensis forest ecosystem to climate change based on Biome-BGC model and tree rings. Acta Ecologica Sinica, 2018, 38(20): 7435-7446.
- Zhang, Y., M. Huang, and J. Lian. 2015. Spatial distributions of optimal plant coverage for the dominant tree and shrub species along a precipitation gradient on the central Loess Plateau. Agricultural and Forest Meteorology 206:69-84.
- Du, L., Y. Zeng, L. Ma, C. Qiao, H. Wu, Z. Su, and G. Bao. 2021. Effects of anthropogenic revegetation on the water and carbon cycles of a desert steppe ecosystem. Agricultural and Forest Meteorology 300:108339
- Xu, X., G. Yang, Y. Tan, X. Tang, H. Jiang, X. Sun, Q. Zhuang, and H. Li. 2017. Impacts of land use changes on net ecosystem production in the Taihu Lake Basin of China from 1985 to 2010. Journal of Geophysical Research: Biogeosciences 122:690-707.
- White, M. A., P. E. Thornton, S. W. Running, and R. R. Nemani. 2000. Parameterization and Sensitivity Analysis of the BIOME-BGC Terrestrial Ecosystem Model: Net Primary Production Controls. Earth Interactions 4:1-85.

Table S3. LULC conversion in Beijing between 2000 and 2015 (km²)

LULC in 2000	LULC in 2015					Loss	Loss rate/%	
	Forest	Grassland	Wetland	Cropland	Urban			
Forest	7890.52	15.12	4.41	52.83	65.95	8028.83	138.31	1.72
Grassland	68.23	649.03	5.63	83.36	78.52	884.77	235.74	26.64
Wetland	32.62	41.03	264.23	65.35	70.32	473.54	209.31	44.20
Cropland	364.76	129.42	32.95	3300.31	990.35	4817.79	1517.48	31.50
Urban	6.16	10.00	4.43	14.28	2166.00	2200.88	34.88	1.58
Sum	8362.29	844.60	311.65	3516.13	3371.14			
Gain	471.78	195.57	47.42	215.82	1205.13			
Gain rate/%	5.88	22.10	10.01	4.48	54.76			

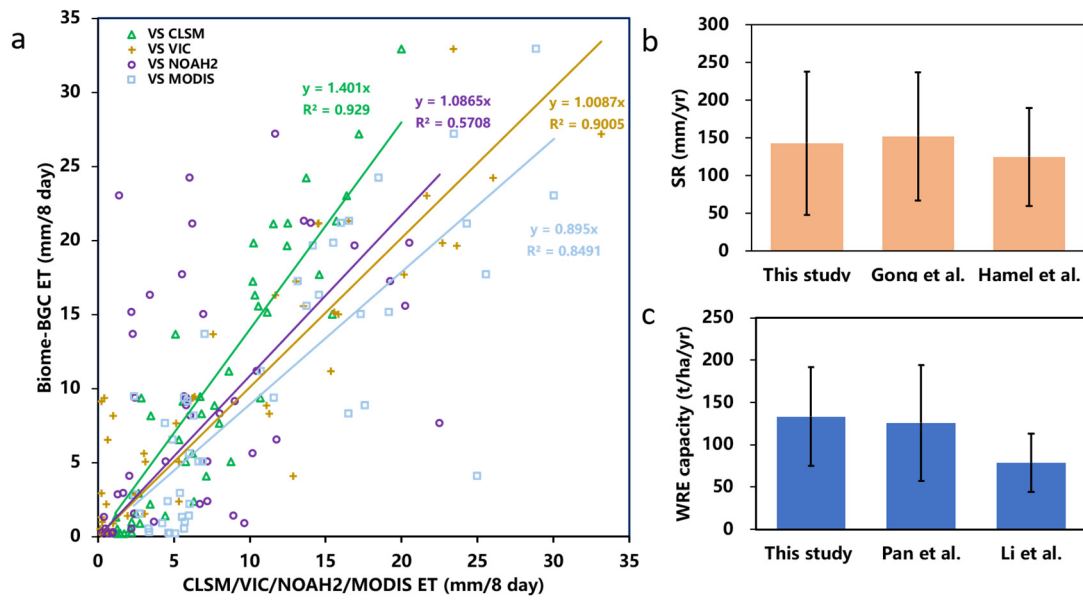


Figure S2. a) Comparison of Biome-BGC ET vs CLSM, VIC, NOAH2 and MODIS ET; b) Comparison of simulated SR from this study and that estimated based on the method of Gong et al. (2017) and Hamel et al. (2020); c) Comparison of simulated WRE from this study and that from Pan et al. (2021) and Li et al. (2000).

- Gong, S. H., Y. Xiao, Y. Xiao, L. Zhang, and Z. Y. Ouyang. 2017. Driving forces and their effects on water conservation services in forest ecosystems in China. Chinese Geographical Science 27:216-228.
- Hamel, P., J. Valencia, R. Schmitt, M. Shrestha, T. Piman, R. P. Sharp, W. Francesconi, and A. J. Guswa. 2020. Modeling seasonal water yield for landscape management: Applications in Peru and Myanmar. Journal of Environmental Management 270:110792.
- Pan, T.; Zuo, L.; Zhang, Z.; Zhao, X.; Sun, F.; Zhu, Z.; Liu, Y. Impact of Land Use Change on Water Conservation: A Case Study of Zhangjiakou in Yongding River. Sustainability 2021, 13, 22. <https://doi.org/10.3390/su13010022>
- LI Y Y, FAN J H, LIAO Y. Analysis of spatial and temporal differences in water conservation function in Zhangjiakou based on the InVEST model. Pratacultural Science, 2020, 37(7): 1313-1324.

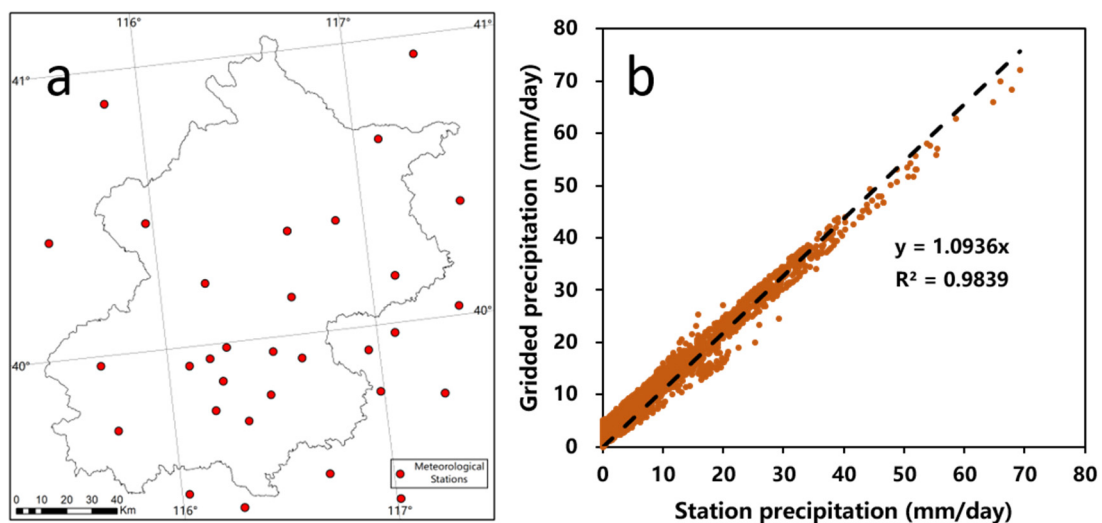


Figure S3. a) Spatial distribution of meteorological stations; b) Comparison of gridded precipitation vs station observed precipitation (mm/day).

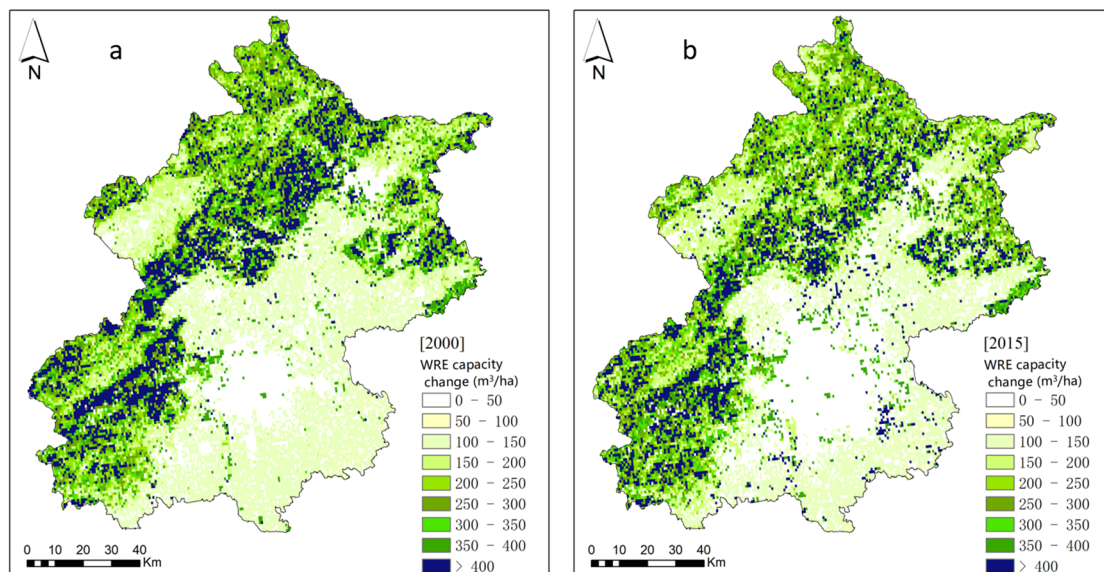


Figure S4. Spatial distribution of WRE capacity (m^3/ha) in a) 2000 and b) 2015.

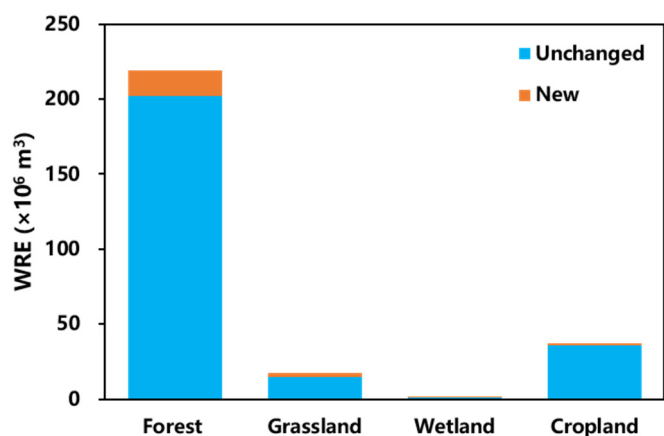


Figure S5. The volume of WRE ($\times 10^6 \text{ m}^3$) in 2015 contributed by different LULCs.

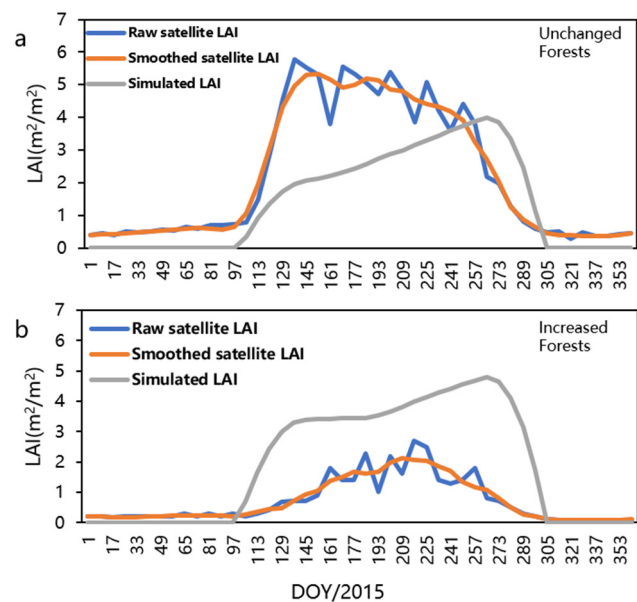


Figure S6. The comparisons of three LAIs among a) unchanged forests and b) increased forests.

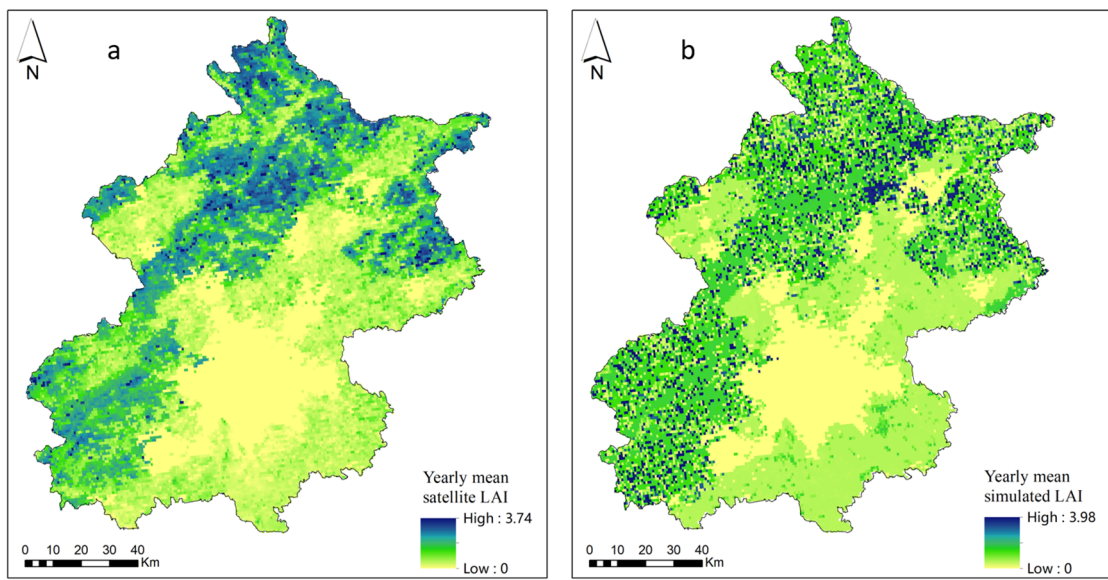


Figure S7. The comparisons of yearly mean smoothed satellite LAI VS simulated LAI in 2015.

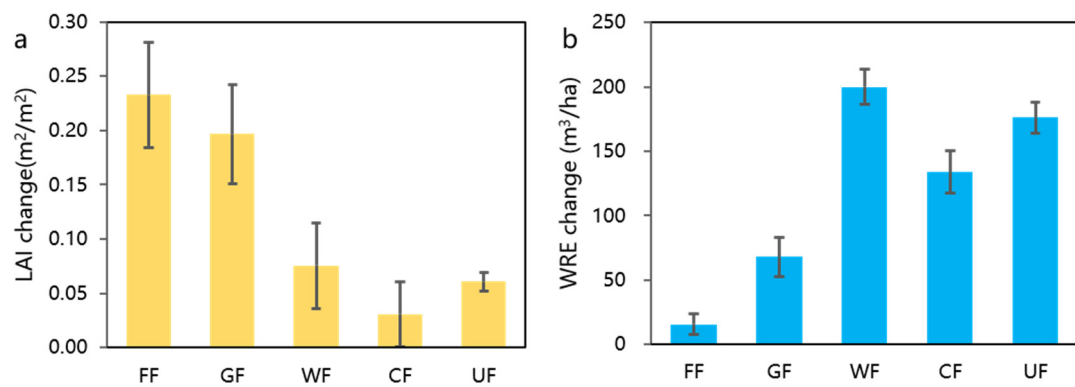


Figure S8. LAI and WRE change across unchanged and increased forests between 2000 and 2015.